

# Discriminating Detection between $Mg^{2+}$ and $Ca^{2+}$ by Fluorescent Signal from Anthracene Aromatic Amide Moiety

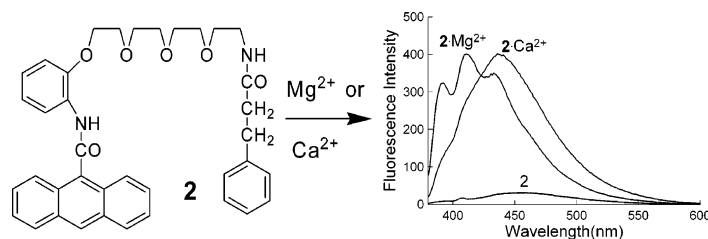
Jeongsik Kim,<sup>†</sup> Tatsuya Morozumi,<sup>‡</sup> and Hiroshi Nakamura<sup>\*‡</sup>

Division of Environmental Material Science, Graduate School of Environmental Science, Hokkaido University, Sapporo, Hokkaido 060-0810, Japan, and Section of Materials Science, Research Faculty of Environmental Earth Science, Hokkaido University, Sapporo, Hokkaido 060-0810, Japan

nakamura@ees.hokudai.ac.jp

Received June 29, 2007

## ABSTRACT



Novel fluorescent reagents 1 and 2 were synthesized. In the absence of metal ions, the fluorescence emissions of these compounds were quite weak, but their intensities were much greater in the presence of alkaline earth metal ions. The peak shape and maximum wavelength of the emission of the complex with  $Mg^{2+}$  differed from those of  $Ca^{2+}$  and other alkaline earth metal ions. The peak wavelength difference was 30 nm.

Because of their high sensitivity and selectivity, crown ethers<sup>1</sup> and polyethers<sup>2</sup> with fluorescent detecting moieties are useful as chemical sensors for the detection and characterization of alkali and alkaline earth metal cations. A particularly

important target in this field is the design and development of chemosensors for analytical use. Although  $Na^+$ ,  $K^+$ ,  $Mg^{2+}$ ,  $Ca^{2+}$ ,  $Fe^{2+}$ , and  $Hg^{2+}$  are well-known to play critical roles in environmental systems, only a few examples of chemosensors for discriminating between  $Mg^{2+}$  and  $Ca^{2+}$  have been reported.<sup>3</sup> The similar chemical properties of  $Mg^{2+}$  and  $Ca^{2+}$  makes differential detection difficult.

A reliable analytical method with use of EDTA is known to be able to determine the concentration of  $Mg^{2+}$  and  $Ca^{2+}$  ions in solution. But EDTA does not show a selectivity for the two cations, and forms two stable complexes. To evaluate the concentration of  $Ca^{2+}$ ,  $Mg^{2+}$  must be removed from the

<sup>†</sup> Division of Environmental Material Science, Graduate School of Environmental Science.

<sup>‡</sup> Section of Materials Science, Research Faculty of Environmental Earth Science.

(1) (a) Fabbrizzi, L.; Poggi, A. *Chem. Soc. Rev.* **1995**, 197. (b) de Silva, A. P.; Gunaratne, H. Q. N.; Gunnlaugsson, T.; Huxley, A. J. M.; McCoy, C. P.; Rademacher, J. T.; Rice, T. E. *Chem. Rev.* **1997**, 97, 1515. (c) Valeur, B.; Leray, I. *Coord. Chem. Rev.* **2000**, 205, 3. (d) McQuade, D. T.; Pullen, A. E.; Swager, T. M. *Chem. Rev.* **2000**, 100, 2537.

(2) (a) McSkimming, G.; Tucker, J. H. R.; Bouas-Laurent, H.; Desvergne, J.-P. *Angew. Chem., Int. Ed.* **2000**, 39, 2167. (b) Nabeshima, T.; Hashiguchi, A.; Saiki, T.; Akine, S. *Angew. Chem., Int. Ed.* **2002**, 41, 481. (c) Nabeshima, T.; Yoshihira, Y.; Saiki, T.; Akine, S.; Horn, E. *J. Am. Chem. Soc.* **2003**, 125, 28. (d) Ames, J. B.; Hendricks, K. B.; Strahl, T.; Huttner, I. G.; Hamasaki, N.; Thorner, J. *Biochemistry* **2000**, 39, 12149. (e) Watanabe, S.; Ikishima, S.; Matsuo, T.; Yoshida, K. *J. Am. Chem. Soc.* **2001**, 123, 8402. (f) Cha, N. R.; Moon, S. Y.; Chang, S.-K. *Tetrahedron Lett.* **2003**, 44, 8265. (g) Momotake, A.; Arai, T. *Tetrahedron Lett.* **2003**, 44, 7277. (h) Kakizawa, Y.; Akita, T.; Nakamura, H. *Chem. Lett.* **1993**, 1671. (i) Tahara, R.; Hasebe, K.; Nakamura, H. *Chem. Lett.* **1995**, 753.

(3) (a) Arunkumar, E.; Chithra, P.; Ajayaghosh, A. *J. Am. Chem. Soc.* **2004**, 126, 6590. (b) Youngblood, W. J.; Gryko, D. T.; Lammi, R. K.; Bocian, D. F.; Holten, D.; Lindsey, J. S. *J. Org. Chem.* **2002**, 67, 2111. (c) Arunkumar, E.; Ajayaghosh, A.; Daub, J. *J. Am. Chem. Soc.* **2005**, 127, 3156. (d) Ajayaghosh, A.; Arunkumar, E.; Daub, J. *J. Am. Chem. Soc.* **2002**, 41, 1766. (e) Ajayaghosh, A. *Acc. Chem. Res.* **2005**, 38, 449. (f) Ajayaghosh, A.; Arunkumar, E.; Daub, J. *Angew. Chem., Int. Ed.* **2002**, 41, 1766. (g) Suzuki, Y.; Morozumi, T.; Nakamura, H.; Shimomura, M.; Hayashita, T.; Bartsch, R. A. *J. Phys. Chem. B* **1998**, 102, 7910.

system as  $\text{Mg}(\text{OH})_2$  in high pH solution. If this differentiation is able to be achieved in one step, it will be of great advantage for a fast and reliable analysis.

In our previous work, linear polyethers with fluorescent substituents (e.g.,  $N,N'$ -[oxybis(3-oxapentamethyleneoxy)-2-phenyl]bis(9-anthracenecarboxamide)) have been synthesized and fluorescence “Off–On” behaviors for alkaline earth metal ions were reported.<sup>4</sup> The twisted intramolecular charge transfer (TICT) quenching process was effectively controlled by formation of a complex with alkaline earth metal ions ( $\text{Ca}^{2+}$ ,  $\text{Sr}^{2+}$ , or  $\text{Ba}^{2+}$ ). These results suggested that a torsion angle between the carbonyl group of the amide bond and a plane of the anthracene ring plays an important role on TICT action. It occurred to us that the difference in ionic radii between  $\text{Mg}^{2+}$  and  $\text{Ca}^{2+}$  can vary the torsion angle in the complex structure. This variation will be reflected in the fluorescence spectrum as a feature and a position of fluorescence maximum. However, the previous work indicated that the emission of complexation with  $\text{Mg}^{2+}$  was weak and gave no remarkable spectral changes compared to those of other cations. This suggested that the anthracene aromatic amide moiety was too large to stop a twisted motion of another side of anthracene for the  $\text{Mg}^{2+}$  complex in the excited state. In the present work, compact and effective “stoppers”, *n*-propyl and ethyl benzene moieties, were chosen. We also recognized that the best binding site is constructed with tetraethylene oxide units. On the basis of these ideas, we synthesized fluorescent reagents **1** and **2**.

Herein, we report the results of novel fluorescent chemosensors that can distinguish between  $\text{Mg}^{2+}$  and  $\text{Ca}^{2+}$  using a fluorescence emission spectroscopy.

Chemosensors **1** and **2** (Figure 1) were synthesized in the usual manner (see the Supporting Information).<sup>4,5</sup> Their

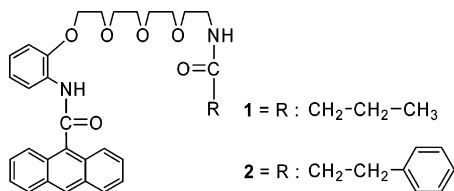


**Figure 1.** Structures of **1** and **2**.

structures and purities were respectively confirmed by using  $^1\text{H}$  NMR and elemental analyses (see the Supporting Information). Fluorescence and UV spectra were measured at 25 °C (RF-5300PC, UV-2400PC; Shimadzu Corp.). The concentration of these fluorescent reagents was  $1 \times 10^{-5}$  mol/dm<sup>3</sup> in purified acetonitrile. Alkaline earth metal cations were added to the solution as perchlorate salts.

Figure 2 shows the fluorescence spectra of **2** as a function of the  $\text{Mg}^{2+}$  and  $\text{Ca}^{2+}$  concentrations in acetonitrile. Fluorescence emissions from the anthracene moieties were quite

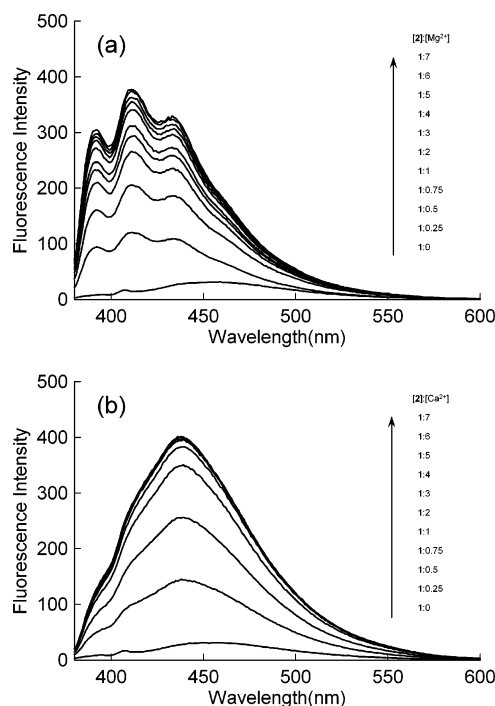


**Figure 2.** Fluorescence spectra of **2** and its  $\text{Mg}^{2+}$  (a) and  $\text{Ca}^{2+}$  (b) complexes.

weak in the absence of any metal ions, such as compounds reported previously.<sup>4,5</sup> The  $\lambda_{\text{max}}$  of the weak emission of **2** was 460 nm, which was attributed to the exciplex emission of anthracene and benzene unit attached to the anthracene. This observation was supported by the fluorescence spectrum of free **1**. The fluorescence spectra of  $\text{2}\cdot\text{Mg}^{2+}$  showed increasing intensity and vibrational splitting at around 410 nm (Figure 2a). These peaks were attributed to emissions from the anthracene moiety. This result indicates that no charge transfer interaction existed between the anthracene and the carbonyl group. On the other hand, in the case of the  $\text{Ca}^{2+}$  complex, the identical increase of fluorescence intensity was also observed at around 440 nm. The peak feature and wavelength at the peak maximum differed from those of the  $\text{Mg}^{2+}$  complex. This difference allowed a discriminating detection between  $\text{Mg}^{2+}$  and  $\text{Ca}^{2+}$  by means of fluorescence spectroscopy.

The fluorescence behavior of **1** or **2** can be explained as follows. The ionic size of  $\text{Mg}^{2+}$  was fitted for a binding site consistent with CO-NH-Ph-OR. Therefore, the torsion angle remained perpendicular (Figure 3). On the other hand, the ionic size of  $\text{Ca}^{2+}$  is too large to interact with this site. The carbonyl group must be twisted to the anthracene ring at the binding event to avoid a steric repulsion. This torsion motion of the carbonyl group caused the charge transfer interaction for the anthracene ring. Consequently, fluorescence spectra of  $\text{2}\cdot\text{Ca}^{2+}$  exhibited a structureless and longer wavelength. This “Off–On” phenomenon was elucidated as the following pathway: the fluorescence emission from the anthracene moiety was quenched by the TICT process at the aromatic amide bond. The quenching mode was inhibited by the

(4) Morozumi, T.; Anada, T.; Nakamura, H. *J. Phys. Chem. B* **2001**, *105*, 2923.

(5) Morozumi, T.; Hiraga, H.; Nakamura, H. *Chem. Lett.* **2003**, *32*, 146.

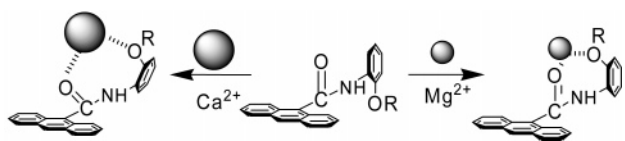


**Figure 3.** Schematic representation of the molecular configuration of  $\text{Mg}^{2+}$  and  $\text{Ca}^{2+}$ . Oxyethylene and terminal benzene moieties were omitted for clarity.

coordination of a metal ion with carbonyl and polyethylene oxide moieties.<sup>4,5</sup>

The “Off–On” responsiveness was evaluated as the intensity enhancement ratio ( $I_{\text{max}}/I_0$ ) at  $\lambda_{\text{max}}$  for each metal cation and is listed in Table 1. The order of  $I_{\text{max}}/I_0$  for **1** was

**Table 1.** Wavelength of Fluorescence Maxima ( $\lambda_{\text{max}}$ ), Fluorescence Intensity Ratios ( $I_{\text{max}}/I_0$ ) at  $\lambda_{\text{max}}$ , and Complex Formation Constants ( $\log K$ )

		$\text{Mg}^{2+}$	$\text{Ca}^{2+}$	$\text{Sr}^{2+}$	$\text{Ba}^{2+}$
<b>1</b>	$\lambda_{\text{max}}$	411 nm	438 nm	438 nm	438 nm
	$I_{\text{max}}/I_0$	16.4	15.1	12.1	5.8
	$\log K$	4.89	5.67	4.95	4.68
<b>2</b>	$\lambda_{\text{max}}$	411 nm	438 nm	439 nm	440 nm
	$I_{\text{max}}/I_0$	28.8	14.9	10.2	5.9
	$\log K$	5.13	6.21	5.35	4.55

$\text{Mg}^{2+}$  (16.4) >  $\text{Ca}^{2+}$  (15.1) >  $\text{Sr}^{2+}$  (12.1) >  $\text{Ba}^{2+}$  (5.8). The order of  $I_{\text{max}}/I_0$  for **2** was  $\text{Mg}^{2+}$  (28.8) >  $\text{Ca}^{2+}$  (14.9) >  $\text{Sr}^{2+}$  (10.2) >  $\text{Ba}^{2+}$  (5.9). The  $I_{\text{max}}/I_0$  of  $\text{Mg}^{2+}$  for **2** obtained as an approximately 2-fold larger value than that of  $\text{Ca}^{2+}$ . This large value is due to the low intensity of free compound

emission at  $\lambda_{\text{max}}$  of the  $\text{Mg}^{2+}$  complex. In comparison to the  $I_{\text{max}}/I_0$  value of **1** and **2** for  $\text{Mg}^{2+}$ , a terminal ethylbenzene in **2** played an effective role in stopping the twisted motion of the anthracene ring compared with that of the *n*-propyl group. The complex formation constant ( $\log K$ ) was evaluated from the titration curve of Abs. vs  $[\text{M}^{2+}]$  by means of a nonlinear least-squares curve-fitting method (Marquardt’s method).<sup>6</sup> The complex formation constants ( $\log K$ ) of **1** and **2** were evaluated from the spectral change that occurred upon the addition of metal ions, and all complexes formed 1:1 stoichiometry. Those values are listed in Table 1. In the alkaline earth cations,  $\text{Ca}^{2+}$  showed the best affinity with **1** and **2**, as indicated also by other chemosensors.<sup>4,5</sup>

Fluorescence spectral data showed a structural change in **1** and **2** upon complexation with metal cations. To clarify the effect of the addition of metal cations, <sup>1</sup>H NMR examination was carried out in acetonitrile-*d*<sub>3</sub> at 30 °C. The spectra of **2** before (a) and after addition of  $\text{Ca}^{2+}$  (b) and  $\text{Mg}^{2+}$  (c) are shown in Figure 4 as a typical result. Peak assignments were determined by using H–H COSY and NOESY 2D spectra. Regarding the complexation of **2** with  $\text{Ca}^{2+}$ , oxyethylene proton peaks *f–h* shifted to low magnetic field ( $\Delta\delta = 0.39$ – $0.56$  ppm) because of the reduction of electron density by the coordinated cations in the oxygen atoms. On the other hand, the proton peaks *a–c* of **2** showed no particular shift tendency; moreover, the shift values were small ( $\Delta\delta = -0.27$  to  $0.27$  ppm) because of the weak interaction of the oxygen atom beside *b* and *c* to the metal ions.

Amide proton *m* showed low magnetic shift changes ( $\Delta\delta = 0.83$  ( $\text{Mg}^{2+}$ ) and  $0.66$  ( $\text{Ca}^{2+}$ )). In the  $\text{Mg}^{2+}$  complex, the chemical shift change was about 0.17 ppm lower than that of the  $\text{Ca}^{2+}$  complex. Another amide proton **1** exhibited similar results ( $\Delta\delta = 1.52$  ( $\text{Mg}^{2+}$ ) and  $0.89$  ( $\text{Ca}^{2+}$ ), respectively) to those of *m*, which suggests that the electronic

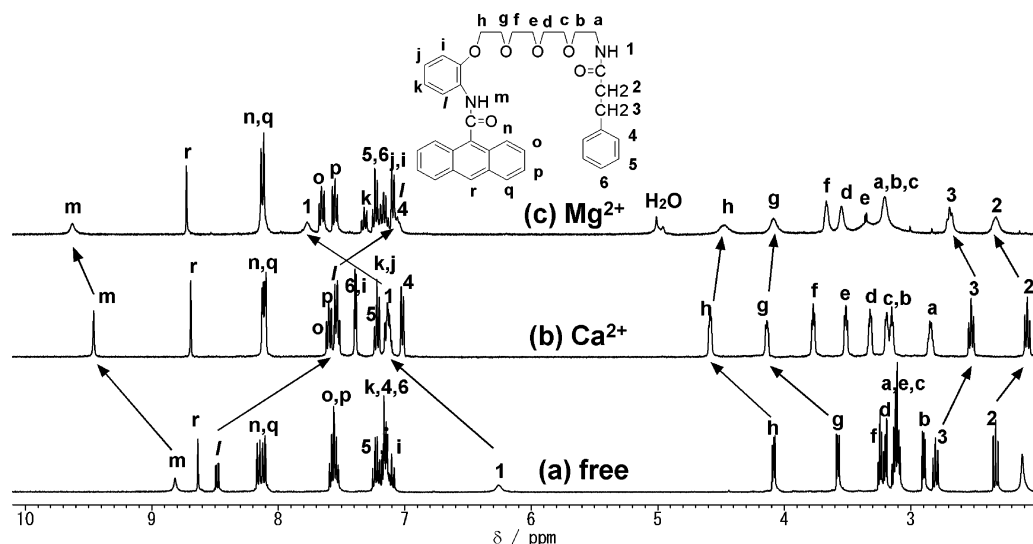


**Figure 4.** <sup>1</sup>H NMR spectra of **2**-free (a), **2**· $\text{Ca}^{2+}$  (b), and **2**· $\text{Mg}^{2+}$  (c).

interaction between  $\text{Mg}^{2+}$  and the carbonyl group in **2** was stronger than that of  $\text{Ca}^{2+}$ ,  $\text{Sr}^{2+}$ , and  $\text{Ba}^{2+}$ .

In contrast to proton *m* and **1**, a high-magnetic chemical shift of proton *l* ( $\Delta\delta = -1.41$  ( $\text{Mg}^{2+}$ ) and  $-0.93$  ( $\text{Ca}^{2+}$ )) was induced upon complexation. These observations of  $^1\text{H}$  NMR indicate that  $\text{Mg}^{2+}$  bound ligand **1** or **2** more tightly than  $\text{Ca}^{2+}$  at the carbonyl group of the aromatic amide. On the basis of fluorescence and  $^1\text{H}$  NMR studies, a plausible complex structure of  $\mathbf{2}\cdot\text{Mg}^{2+}$  in the ground state is illustrated in Figure 5.

In summary, we have shown that fluorescence spectra of the **1** or  $\mathbf{2}\cdot\text{Mg}^{2+}$  complex have different spectral shapes from those of  $\text{Ca}^{2+}$ ,  $\text{Sr}^{2+}$ , and  $\text{Ba}^{2+}$ . The fluorescence spectra of **1** and **2** showed structured anthracene-like peaks at around 410 nm for the  $\text{Mg}^{2+}$  complex, and they showed broad peaks at around 440 nm for  $\text{Ca}^{2+}$ ,  $\text{Sr}^{2+}$ , and  $\text{Ba}^{2+}$  complexes. The present chemosensors **1** and **2** will be useful to discriminate  $\text{Mg}^{2+}$  with use of fluorescence spectroscopy.

(6) Marquardt, D. W. *J. Soc. Ind. Appl. Math.* **1963**, *11*, 431.

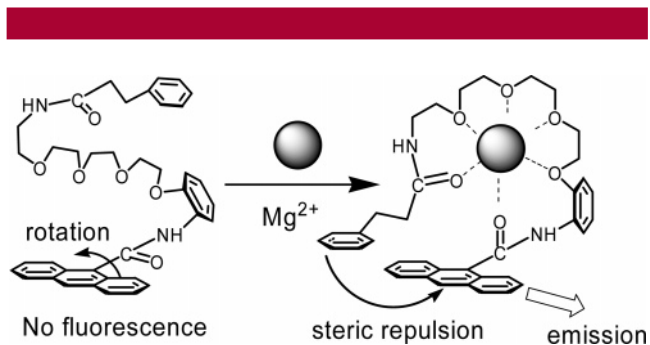


**Figure 5.** Schematic representation of the proposed structural change of **2** after the addition of  $\text{Mg}^{2+}$  in the ground state.

**Supporting Information Available:** Fluorescence spectra and characterization data of **1** and **2**. This material is available free of charge via the Internet at <http://pubs.acs.org>.

OL701976X